Original Article

Diagnostic efficacy of the contrast-enhanced ultrasound thyroid imaging reporting and data system classification for benign and malignant thyroid nodules

Yu-Ping Yang[#]^, Guo-Li Zhang[#], Hong-Lian Zhou, Hai-Xia Dai, Xing Huang, Li-Juan Liu, Jun Xie, Jie-Xin Wang, Hua-Juan Li, Xin Liang, Qian Yuan, Yan-Hao Zeng, Xiao-Hong Xu

Department of Ultrasound, Affiliated Hospital of Guangdong Medical University, Zhanjiang, China

Contributions: (I) Conception and design: YP Yang, GL Zhang; (II) Administrative support: XH Xu; (III) Provision of study materials or patients: YP Yang, HL Zhou, HX Dai, X Huang, JX Wang, LJ Liu, J Xie; (IV) Collection and assembly of data: GL Zhang, YP Yang; (V) Data analysis and interpretation: GL Zhang, YP Yang; (VI) Manuscript writing: All authors; (VII) Final approval of manuscript: All authors.

[#]These authors contributed equally to this work as co-first authors.

Correspondence to: Xiao-Hong Xu, MD. Department of Ultrasound, Affiliated Hospital of Guangdong Medical University, 57 Southern Renmin Avenue, Xiashan District, Zhanjiang 524000, China. Email: 13828297586@139.com.

Background: The contrasted-enhanced ultrasound thyroid imaging reporting and data system (CEUS TI-RADS) is the first international risk stratification system for thyroid nodules based on conventional ultrasound (US) and CEUS. This study aimed to evaluate the diagnostic efficacy of CEUS TI-RADS for benign and malignant thyroid nodules and to assess the related interobserver agreement.

Methods: The study recruited 433 patients who underwent thyroid US and CEUS between January 2019 and June 2023 at the Affiliated Hospital of Guangdong Medical University. A retrospective analysis of 467 thyroid nodules confirmed by fine-needle aspiration (FNA) and/or surgery was performed. Further, a CEUS TI-RADS classification was assigned to each thyroid nodule based on the CEUS TI-RADS scoring criteria for the US and CEUS features of the nodule. The nodules were grouped based on their sizes as follows: size ≤1 cm, group A; size >1 and ≤4 cm, group B; and size >4 cm, group C. Multivariate logistic regression was used to analyze independent risk factors for malignant thyroid nodules. Pathological assessment was the reference standard for establishing the sensitivity (SEN), specificity (SPE), accuracy (ACC), positive predictive value (PPV), and negative predictive value (NPV) of CEUS TI-RADS in diagnosing malignant thyroid nodules. The area under the curve (AUC) in the receiver operating characteristic (ROC) curve analysis was used to compare the diagnostic efficacy of the scoring system in predicting malignancy in three groups of nodules. The intragroup correlation coefficient (ICC) was adopted to assess the interobserver agreement of the CEUS TI-RADS score.

Results: Out of the 467 thyroid nodules, 262 were malignant and 205 were benign. Logistic regression analysis revealed that the independent risk factors for malignant thyroid nodules included punctate echogenic foci (P<0.001), taller-than-wide shape (P=0.015), extrathyroidal invasion (P=0.020), irregular margins/lobulation (P=0.036), hypoechoicity on US (P=0.038), and hypoenhancement on CEUS (P<0.001). The AUC for the CEUS TI-RADS in diagnosing malignant thyroid nodules was 0.898 for all nodules, 0.795 for group A, 0.949 for group B, and 0.801 for group C, with the optimal cutoff values of the CEUS TI-RADS being 5 points, 6 points, 5 points, and 5 points, respectively. Among these groups of nodules, group B had the highest AUC, with the SEN, SPE, ACC, PPV, and NPV for diagnosing malignant nodules being 95.9%,

^ ORCID: 0000-0001-9889-8389.

88.1%, 92.8%, 92.6%, and 93.2%, respectively. The ICC of the CEUS TI-RADS classification between senior and junior physicians was 0.862 (P<0.001).

Conclusions: In summary, CEUS TI-RADS demonstrated significant efficacy in distinguishing thyroid nodules. Nonetheless, there were variations in its capacity to detect malignant nodules across diverse sizes, and it demonstrate optimal performance in 1- to 4-cm nodules. These findings may serve as important insights for clinical diagnoses.

Keywords: Contrasted-enhanced ultrasound thyroid imaging reporting and data system (CEUS TI-RADS); thyroid nodules; malignancy; ultrasound (US); contrasted-enhanced ultrasound (CEUS)

Submitted Mar 07, 2024. Accepted for publication Jun 21, 2024. Published online Jul 30, 2024.
doi: 10.21037/qims-24-457
View this article at: https://dx.doi.org/10.21037/qims-24-457

Introduction

Thyroid nodules are distinct lesions inside the thyroid gland that differ radiologically from the surrounding thyroid parenchyma. Their etiology ranges from common inflammatory responses and hyperplasia to substantial changes in the tumor. In recent decades, nodule detection has significantly improved, driven by the development and widespread availability of high-resolution ultrasound (US) technology. Thyroid nodules are prevalent, occurring in an estimated 60% of adults (1). Although only approximately 5% of nodules are ultimately found to be malignant (2), the possibility of malignancy is a major concern and timely screening of thyroid nodules is increasingly important to clinicians and patients. Accurate detection of benign and malignant thyroid nodules is a critical element of preoperative US, which can effectively reduce the risk of puncture.

Several US risk stratification systems for thyroid nodules, including the thyroid imaging reporting and data system (TI-RADS) have been introduced by many international organizations, among them the major associations in Chile and Korea, the European Thyroid Association, the American College of Radiology (ACR), and the Chinese Medical Association (CMA) (3-7). Nonetheless, these systems are based on a two-dimensional US assessment of thyroid nodules, which lacks information on blood flow microcirculation and thus make the precise assessment of the nodules difficult. Unlike conventional US, the contrasted-enhanced ultrasound (CEUS) can provide real-time insights into the vascular perfusion and hemodynamics of thyroid nodules, allowing dynamic assessment of microvascularization patterns (8), which is considered a valuable novel approach for identifying benign and malignant nodules (9,10). In recent years, several researchers in China and internationally have examined and characterized the contrast patterns of malignant nodules, such as inhomogeneous enhancement, centripetal or centrifugal enhancement, hypoenhancement, and irregular ring enhancement, of which hypoenhancement is considered to be the main CEUS pattern feature of malignant thyroid nodules (11,12). In addition, CEUS has nonnegligible clinical value for the prediction of cervical lymph node metastasis of thyroid malignant nodules. For cervical lymph node metastases, Liu *et al.* (13) found that the larger diameter of the thyroid tumor, the closer the thyroid tumor is to the thyroid capsule, or the greater the number of neovascularizations, the higher the probability of cervical lymph node metastasis is. All these factors represent channels for the invasion and metastasis of cervical lymph nodes. Additionally, it has been reported that the CEUS features of metastatic lymph nodes in the neck typically show centripetal enhancement, heterogeneous enhancement, and perfusion defects (14). Through univariate and multivariate logistic regression analyses, Ruan *et al.* (15) discovered that nodule composition, echogenicity, shape, margins, echogenic foci, and extrathyroidal extension on US, as well as the direction of enhancement, peak intensity, and circumferential enhancement on CEUS, are important predictors of thyroid carcinoma. However, previous research has also found that the size of thyroid nodules influences vascular development and visualization and the biological behavior and prognosis of thyroid nodules (16-19), resulting in variability in clinical decisions. In this study, we investigated the diagnostic value of CEUS TI-RADS in nodules of different sizes by using a maximum diameter of nodule of 1 cm and a boundary of 4 cm for more discerning reference information in clinical

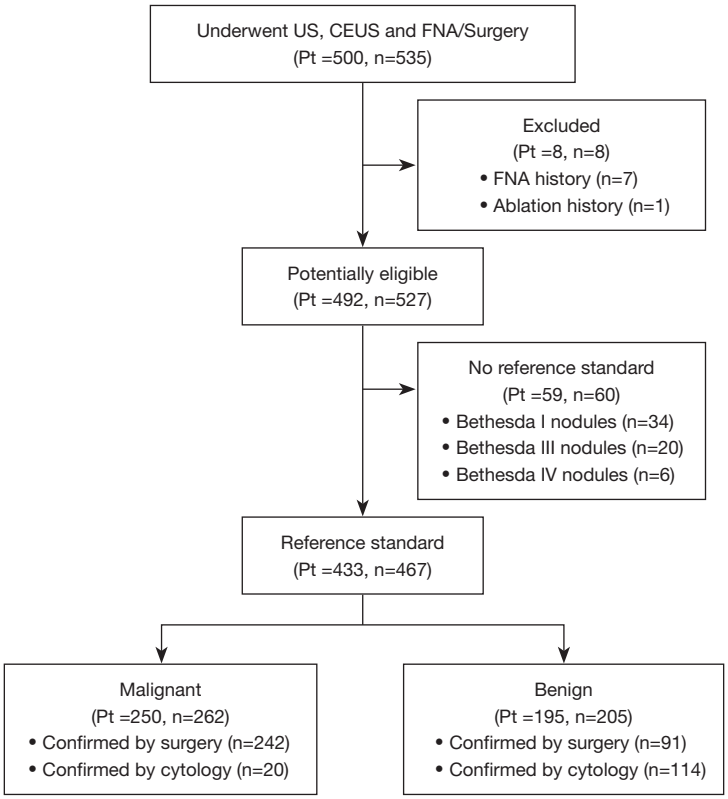

Figure 1 Study flowchart. Out of 433 patients, 400 patients had a single nodule, 32 patients had two thyroid nodules, and 1 patient had three nodules. Out of 262 malignant nodules, 12 patients had 2 malignant nodules. And out of 205 benign nodules, 8 patients had 2 benign nodules and 1 patient had three nodules. Besides, 12 patients had both 1 benign nodule and 1 malignant nodule. US, ultrasound; CEUS, contrast-enhanced ultrasound; FNA, fine-needle aspiration; pt, number of patients; n, number of thyroid nodules.

decision-making.

This study sought to confirm the diagnostic efficacy of CEUS TI-RADS in thyroid nodules and further assess the diagnostic performance of CEUS TI-RADS for thyroid nodules of various sizes. Moreover, the use of CEUS TI-RADS between sonographers of different seniorities was assessed according to the interobserver concordance of CEUS TI-RADS scores. We present this article in accordance with the STARD reporting checklist (available at https://qims.amegroups.com/article/view/10.21037/qims-24-457/rc).

Methods

Ethics statement

This retrospective study was conducted in accordance with the Declaration of Helsinki (as revised in 2013) and was approved by the medical ethics committee of the Affiliated Hospital of Guangdong Medical University (No. PJKT2024-028). Each patient signed the informed consent papers for the CEUS, fine-needle aspiration (FNA), and surgery tests/procedures.

Study population

The inclusion criteria for this study were following: (I) completion of US and CEUS at the Affiliated Hospital of Guangdong Medical University; (II) a final postoperative pathological result or FNA result of Bethesda II, Bethesda Ⅴ, or Bethesda VI based on The Bethesda System for Reporting Thyroid Cytopathology (TBSRTC) (20); and (III) no history of previous treatment, including thyroid surgery, chemotherapy, radiotherapy, or I131 treatment. Meanwhile, the exclusion criteria were as follows: (I) nodules classified as Bethesda I, III, or IV according to TBSRTC and (II) missing final pathologic results. A total of 433 patients who fulfilled the inclusion criteria were included between January 2019 and June 2023 (*Figure 1*).

US					CEUS			
Echogenicity	Shape	Margin	Echogenic foci	Extrathyroidal extension	Direction of enhancement	Peak intensity	Ring enhancement	Composition
Hyper/iso-echoic (0 point)	Wider than taller (0 point)	Smooth or ill-defined (0 point)	No calcification (0 point)	Absent (0 point)	Scattered (0 point)	No enhancement (0 point)	Absent (0 point)	Non-solid (0 point)
			Macrocalcification (1 point)			Iso-enhancement (0 point)		
Hypoechoic /very hypoechoic (1 point)	Taller than wide (1 point)	Irregular or lobulated (1 point)	Rim calcification (1 point)	Present (1 point)	Centripetal /centrifugal (1 point)	Hyper-enhancement (1 point)	Present (1 point)	Solid (1 point)
			Punctate echogenic (2 points)			Hypo-enhancement (1 point)		

The total score for the above US and CEUS characteristics was accumulated to obtain the CEUS TI-RADS classification						
0 point	1 point	2 points	3 points	4 points	5 points	6 points
TR 1	TR 2	TR 3	TR 4A	TR 4B	TR 4C	TR 5
Benign (0%) No biopsy	Not suspicious (3%) No biopsy	Mildly Suspicious (6–7%) Biopsy ≥2.5 cm	Moderately Suspicious (14–17%) Biopsy ≥1.5 cm	Moderately Suspicious (30–38%) Biopsy ≥1.5 cm	Moderately Suspicious (54–73%) Biopsy ≥1.5 cm	Highly Suspicious (92–99%) Biopsy ≥1.0 cm

Figure 2 Chart of the CEUS TI-RADS, with correspondent malignant probabilities and indications for FNA. US, ultrasound; CEUS, contrast-enhanced ultrasound; CEUS TI-RADS, contrasted-enhanced ultrasound thyroid imaging reporting and data system; TR, TI-RADS; FNA, fine-needle aspiration.

Conventional US and CEUS examination

A high-frequency linear probe (Acuson Sequoi, Siemens Healthineers, Erlangen, Germany; Aplio 500, Canon, Tokyo, Japan) was used for each US inspection. SonoVue (Bracco Imaging S.p.A., Milan, Italy), a sulfur-hexafluoride-filled microbubble contrast agent protected by a flexible phospholipid shell, was used as the contrast medium. To create an intravenous access, a 20-G needle was placed into the patient's median cubital vein. The patient was instructed not to swallow after the contrast agent, and 5-mL of saline were combined and mixed until homogenous. Subsequently, 2.4 mL of the suspension was rapidly injected into the median cubital vein while the probe and body posture were kept constant. After injection, the timer on the US machine was set to start. The photographs were stored on the hard disk of the US device, which was constantly monitoring the dynamic perfusion process of the lesion in real-time.

The CEUS TI-RADS classification was assigned to each thyroid nodule based on the CEUS TI-RADS scoring criteria for US and CEUS features of the nodule. These features included size, echogenicity, shape, margin, echogenic foci, and extra-thyroidal invasion in US, as well as enhancement direction, peak intensity, ring enhancement, and composition on CEUS. The nodules were grouped based on their sizes as follows: nodule size ≤1 cm, group A; size >1 cm and size ≤4 cm, group B; and size >4 cm, group C.

To calculate the interobserver concordance of the CEUS TI-RADS scores, 150 thyroid nodule images were randomly selected for individual analysis of the US and CEUS features. Two sonographers performed the analysis. The junior sonographer had experience of 4 years in thyroid ultrasonography, while the senior sonographer had 8 years of experience. Importantly, both sonographers were blinded to the pathologic findings, and nodules were scored and categorized following the CEUS TI-RADS classification criteria. Subsequently, interobserver variability in CEUS TI-RADS scores was retrospectively evaluated. *Figure 2* presents the criteria for the CEUS TI-RADS categories.

Statistical analysis

Statistical analyses were performed on SPSS 27.0 (IBM Corp., Armonk, NY, USA; RRID:SCR_019096) and MedCalc 22.0 (MedCalc Software, Ostend, Belgium; RRID:SCR_015044). Normally distributed measurements are presented as the mean ± standard deviation. Comparisons of categorical variables were performed using

the χ^2 test, and logistic regression was employed to identify independent risk factors predictive of malignant nodules for both US and CEUS characteristics. Receiver operating characteristic (ROC) analysis was used to establish the cutoff values, compute the area under the curve (AUC), and establish 95% confidence intervals (CIs). The sensitivity (SEN), specificity (SPE), accuracy (ACC), positive predictive value (PPV), and negative predictive value (NPV) were measured to assess the diagnostic efficiency of the CEUS TI-RADS system. The significance level was set at P<0.05. Interobserver agreement for CEUS TI-RADS scores was evaluated via the intragroup correlation coefficient (ICC). The agreement was classified as poor (ICC ≤0.50), moderate (0.50< ICC ≤0.75), good (0.75< ICC ≤0.90), or very good (ICC >0.90).

Results

Study population, US, and CEUS features of thyroid nodules

In total, 500 patients with 535 nodules underwent US, CEUS, and FNA/surgery between January 2019 and June 2023. A total of 8 nodules were excluded due to FNA history (n=7) or ablation (n=1). Moreover, 60 nodules, including 34 Bethesda I nodules, 20 Bethesda III nodules, and 6 Bethesda IV nodules were excluded for the lack of reference standard. Finally, 467 nodules from 433 patients were included, among whom 33 had two nodules and 1 patient had 3 nodules. The mean age of all malignant nodules was 45±13 years, and the mean age of benign nodules was 48±13 years. The mean maximum diameter of the nodules was 1.85±0.06 cm (range, 0.50–9.00 cm). Out of the 467 nodules, 262 were malignant and 205 were benign. A total of 242 malignant nodules were diagnosed with the pathologic result, including 234 papillary thyroid carcinomas (PTCs), 6 follicular thyroid carcinomas (FTCs), and 2 medullary thyroid carcinomas (MTCs). A total of 91 benign nodules were surgically confirmed, including 62 nodular goiters, 12 follicular thyroid adenomas (FTAs), 7 cases of Hashimoto thyroiditis, 3 cases of granulomatous thyroiditis, 3 Hürthle cell tumors, 1 ectopic thymus, and 3 noninvasive follicular thyroid neoplasms with papillary-like nuclear features (NIFTPs). The cytologic assessment confirmed 20 malignant and 114 benign nodules, among which 3 were Bethesda V, 17 were Bethesda VI, and 114 were Bethesda II. *Table 1* shows the US and CEUS characteristics of all nodules.

Logistic regression analysis and diagnostic effect of CEUS TI-RADS

As shown by logistic regression analysis, punctate echogenic foci (P<0.001), taller-than-wide shape (P=0.015), extrathyroidal invasion (P=0.020), irregular margins/lobulation (P=0.036), hypoechoicity (P=0.038) on US, and hypoenhancement (P<0.001) on CEUS were the independent risk factors for malignant thyroid nodules (*Table 2*). The nodules were grouped based on their sizes. The diagnostic efficacy of the CEUS TI-RADS classification in differentiating benign and malignant thyroid nodules was examined using ROC analysis (*Figure 3*). The AUC of CEUS TI-RADS for all nodules was 0.898 (95% CI: 0.867–0.924, P<0.001), whereas nodules of the group B obtained excellent performance with an AUC, SEN, SPE, ACC, PPV, and NPV of 0.949 (95% CI: 0.916–0.971; P<0.001), 95.9%, 88.1%, 92.8%, 92.6%, and 93.2%, respectively. Meanwhile, the AUC, SEN, SPE, ACC, PPV, and NPV of ACR-TIRADS for diagnosing malignant thyroid nodules in group B were 0.899 (95% CI:

Table 1 Clinical features of the study population and basic characteristics of the thyroid nodules

Parameter	Benign nodules (n)	Malignant nodules (n)	P value
No. of patients	198	247	
No. of nodules	205	262	
Age (years), mean ± SD	48±13	45±13	0.005
Sex, n (%)			0.072
Male	43 (21.0)	74 (28.2)	
Female	162 (79.0)	188 (71.8)	

Table 1 *(continued)*

Table 1 *(continued)*

Parameter	Benign nodules (n)	Malignant nodules (n)	P value
Nodule size, n (%)			0.002
Size ≤1 cm	69 (33.7)	79 (30.2)	
Size >1 and ≤4 cm	109 (53.2)	170 (64.9)	
Size >4 cm	27 (13.2)	13 (5.0)	
Echogenicity on US, n (%)			<0.001
Hyper/isoechoic	81 (39.5)	12 (4.6)	
Hypoechoic	121 (59.0)	247 (94.3)	
Highly hypoechoic	3 (1.5)	3 (1.1)	
Shape on US, n (%)			<0.001
Wider than taller	166 (81.0)	128 (48.9)	
Taller than wide	39 (19.0)	134 (51.1)	
Margin on US, n (%)			<0.001
Smooth or ill-defined	194 (94.6)	170 (64.9)	
Irregular or lobulated	11 (5.4)	92 (35.1)	
Echogenic foci on US, n (%)			<0.001
No calcification	132 (64.4)	38 (14.5)	
Macrocalcification	38 (18.5)	26 (9.9)	
Rim calcification	3 (1.5)	3 (1.1)	
Punctate echogenic	32 (15.6)	195 (74.5)	
Extrathyroidal extension on US, n (%)			<0.001
Absent	202 (98.5)	198 (75.6)	
Present	3 (1.5)	64 (24.4)	
Enhancement direction on CEUS, n (%)			<0.001
Scattered	44 (21.5)	14 (5.3)	
Centripetal/centrifugal	161 (78.5)	248 (94.7)	
Peak intensity on CEUS, n (%)			<0.001
No/isoenhancement	115 (56.1)	18 (6.9)	
Hypoenhancement	54 (26.3)	224 (85.5)	
Hyperenhancement	36 (17.6)	20 (7.6)	
Ring enhancement on CEUS, n (%)			<0.001
Absent	118 (57.6)	246 (93.9)	
Present	87 (42.4)	16 (6.1)	
Composition on CEUS, n (%)			<0.001
Nonsolid	20 (9.8)	3 (1.1)	
Solid	185 (90.2)	259 (98.9)	

SD, standard deviation; US, ultrasound; CEUS, contrast-enhanced ultrasound.

Table 2 Factors associated with malignancy in thyroid nodules

US and CEUS features	B	SE	P value	OR (95% CI)
Punctate echogenic foci on US	2.12	38.54	<0.001	8.34 (4.27–16.28)
Taller than wide on US	0.80	5.95	0.015	2.22 (1.70–4.20)
Extrathyroidal extension present on US	1.58	5.43	0.020	4.86 (1.29–18.36)
Irregular or lobulated in margin on US	0.90	4.38	0.036	2.46 (1.06–5.70)
Hypoechoic on US	1.05	4.31	0.038	2.86 (1.06–7.72)
Hypoenhancement on CEUS	1.78	17.29	<0.001	5.93 (2.56–13.73)

CEUS, contrast-enhanced ultrasound; SE, standard error; OR, odds ratio; CI, confidence interval; US, ultrasound.

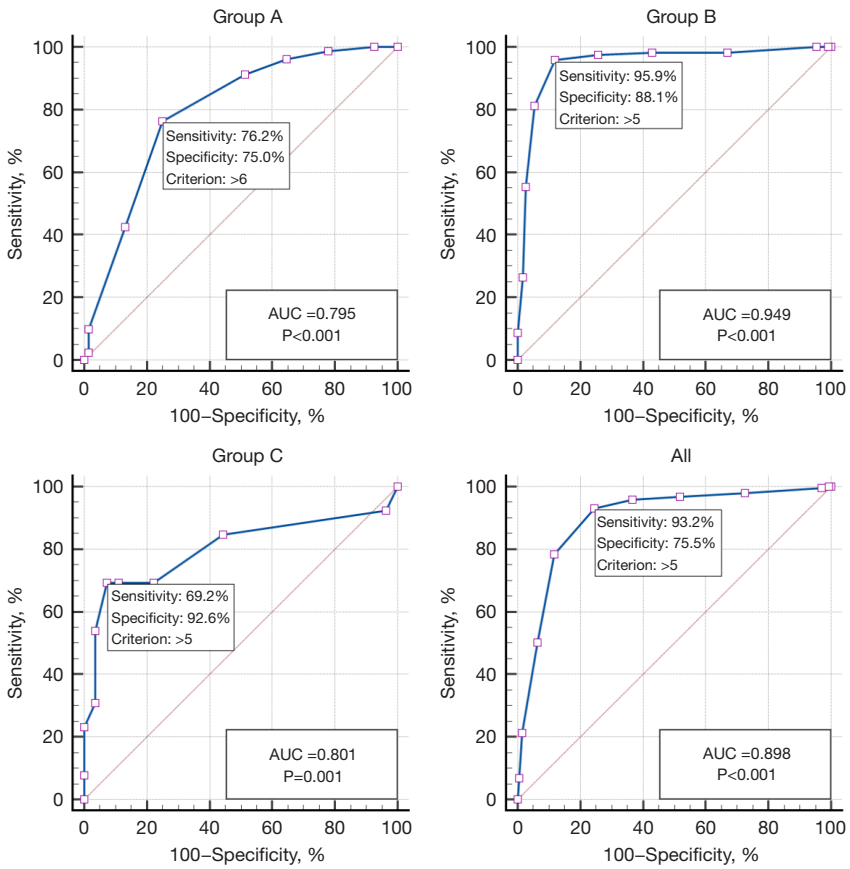

Figure 3 ROC analyses for the diagnostic performance of the CEUS TI-RADS for predicting the malignancy of thyroid nodules in different groups. The nodules were grouped based on their sizes as follows: size ≤1 cm, group A; size >1 and ≤4 cm, group B; and size >4 cm, group C. AUC, area under the curve; ROC, receiver operating characteristic; CEUS TI-RADS, contrasted-enhanced ultrasound thyroid imaging reporting and data system.

0.857–0.942, P<0.001), 91.8%, 88.1%, 90.3%, 92.3%, and 87.3%, respectively. *Table 3* presents the AUC, SEN, SPE, ACC, PPV, and NPV of the CEUS TI-RADS for different groups.

US and CUES characterization of the three groups of thyroid nodules

In group A, echogenicity, shape, and calcification on the

Table 3 Comparison of the diagnostic performances of CEUS TI-RADS in nodules of different sizes

Group	SEN (%)	SPE (%)	ACC (%)	PPV (%)	NPV (%)	AUC (95% CI)	Cutoff	P value
All	93.2	75.5	85.2	83.0	89.0	0.898 (0.867–0.924)	5 points	<0.001
A	76.2	75.0	71.0	67.3	80.5	0.795 (0.721–0.857)	6 points	<0.001
B	95.9	88.1	92.8	92.6	93.2	0.949 (0.916–0.971)	5 points	<0.001
C	69.2	92.6	85.0	81.8	86.2	0.801 (0.644–0.910)	5 points	<0.001

The nodules were grouped based on their size as follows: size ≤1 cm, group A; size >1 and ≤4 cm, group B; and size >4 cm, group C. CEUS TI-RADS, contrasted-enhanced ultrasound thyroid imaging reporting and data system; SEN, sensitivity; SPE, specificity; ACC, accuracy; PPV, positive predictive value; NPV, negative predictive value; AUC, area under the curve; CI, confidence interval.

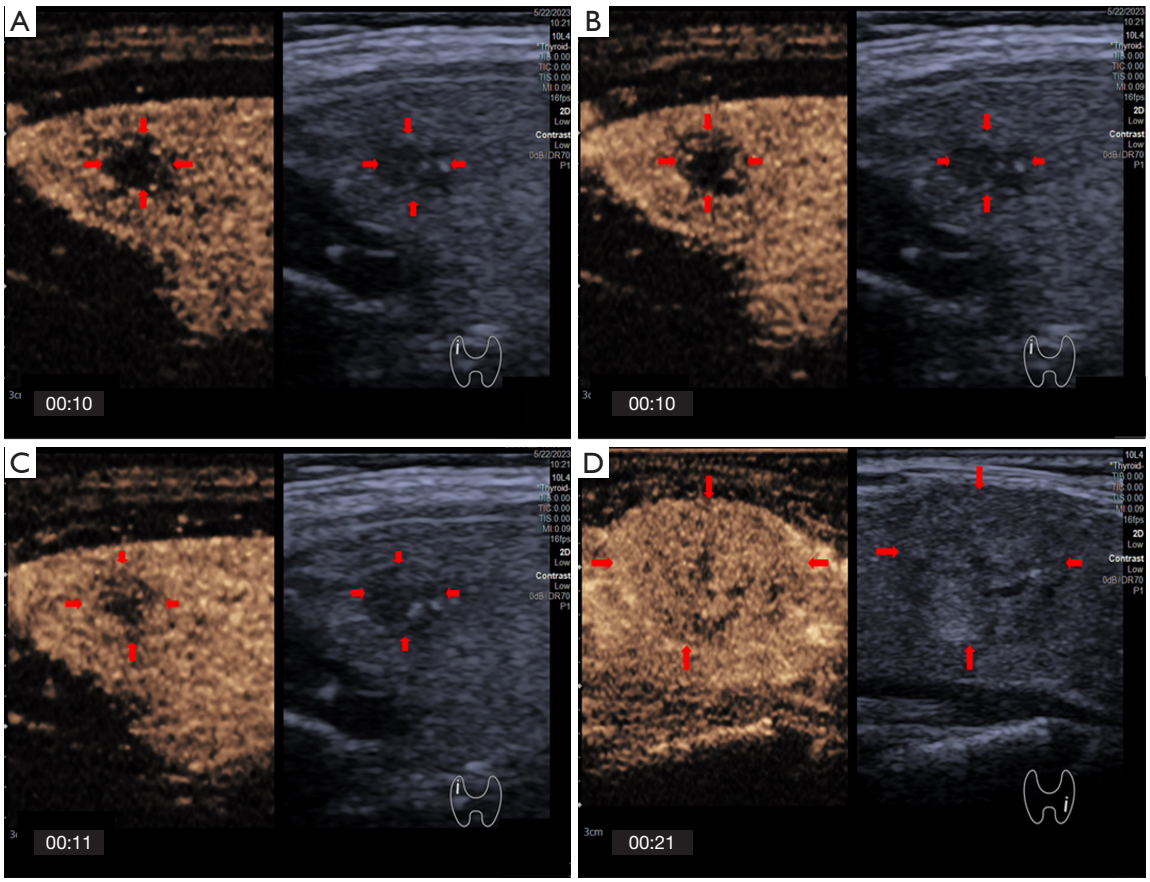

Figure 4 Enhancement direction on CEUS. (A-C) Images showing centripetal enhancement of the same PTC nodule (red arrows) in the right lobe of thyroid gland of a 69-year-old woman. (D) Image of a case of a benign nodule (red arrows) in the left lobe of thyroid gland of a 41-year-old woman showing a feature of scattered enhancement on CEUS. The minutes and seconds after the contrast media injection are indicated by numbers in the bottom left corner of each panel. CEUS, contrast-enhanced ultrasound; PTC, papillary thyroid carcinoma.

US, as well as the direction of enhancement (*Figures 4,5*), peak intensity (*Figure 6*), and composition (*Figure 7*) on CEUS, were statistically different between benign and malignant nodules (P<0.05). On the other hand, margin (P=0.050), extrathyroidal invasion (P=0.306) on US, and ring enhancement (P=0.878) on CEUS were not statistically different between benign and malignant nodules. In group C, margin, calcification, and extra-thyroidal invasion on US, as well as peak intensity, ring enhancement, and composition on CEUS, were statistically different between benign

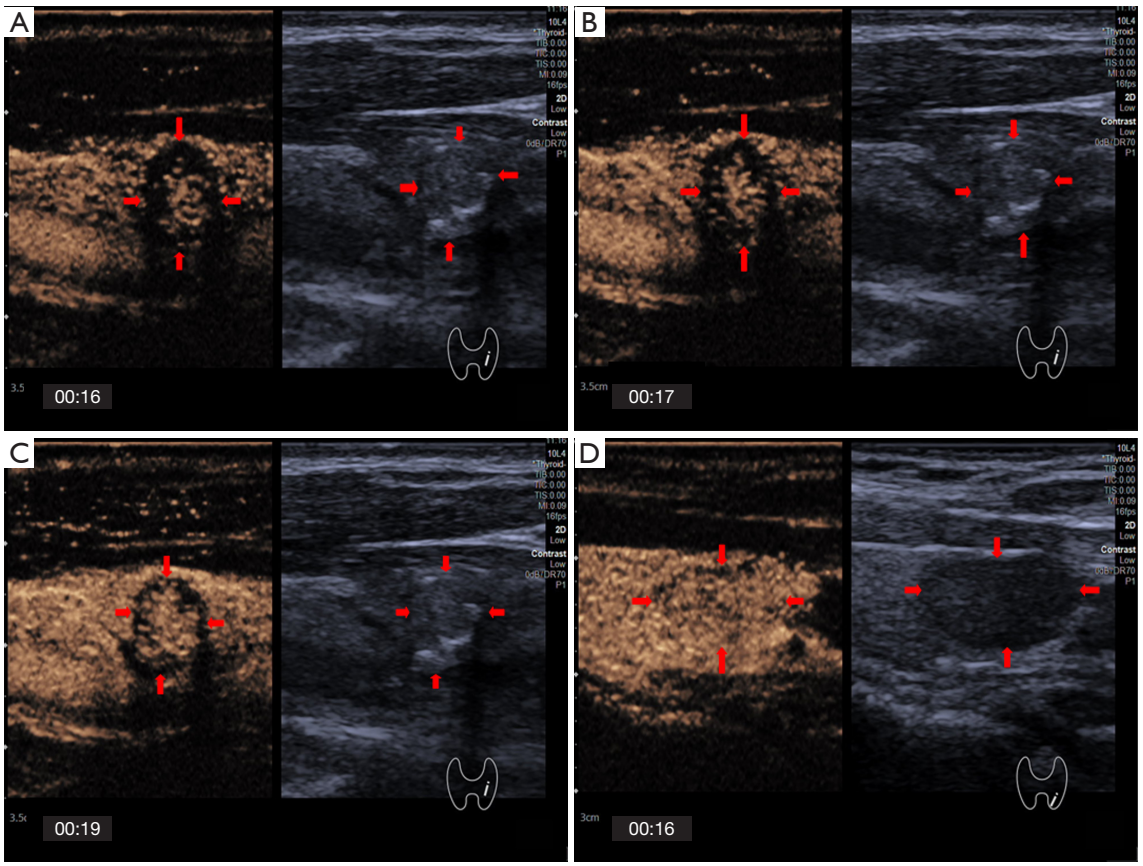

Figure 5 Enhancement direction on CEUS. (A-C) Images of centrifugal enhancement of the same PTC nodule (red arrows) in the left lobe of the thyroid gland of a 69-year-old man. (D) A case of a benign nodule (red arrows) in the left lobe of the thyroid gland of a 65-year-old woman showing the feature of scattered enhancement on CEUS. The minutes and seconds after the contrast media injection are indicated by the numbers in the bottom left corner of each panel. CEUS, contrast-enhanced ultrasound; PTC, papillary thyroid carcinoma.

and malignant nodules (P<0.05), whereas echogenicity (P=0.171), shape (P>0.999) on US, enhancement direction (P=0.845), and composition (P>0.999) on CEUS were not statistically different. In group B, all US and CEUS characteristics were statistically different (P<0.05) (*Table 4*).

Interobserver agreement

The ICC was used to analyze the concordance between the scores of senior and junior sonographers for 150 thyroid nodules. The results indicated that the ICC between senior and junior sonographers for the CEUS TI-RADS score was 0.862 (P<0.001).

Discussion

Currently, US is the preferred screening method for thyroid diseases due to its advantages of noninvasiveness, low cost, lack of radiation, simplicity, and reproducibility. In recent years, US technology in this field has made considerable progress in areas such as CEUS and US elastography. These novel technologies are essential to the differential diagnosis of thyroid nodules.

Zhang *et al.* (21) combined traditional US, shear wave elastography, and *BRAF* V600E mutation status to evaluate nodules with benign FNA results and then compared them with the final pathological results; they found that the diagnostic efficacy of the three combined methods was statistically higher than those of each used alone (P<0.05), suggesting that further clinical decision-making should be considered for any nodule with two or more signs suggestive of US malignancy and with hard US elasticity. Ruan *et al.* (15) pioneered the development of CEUS TI-RADS by combining conventional US with CEUS, and

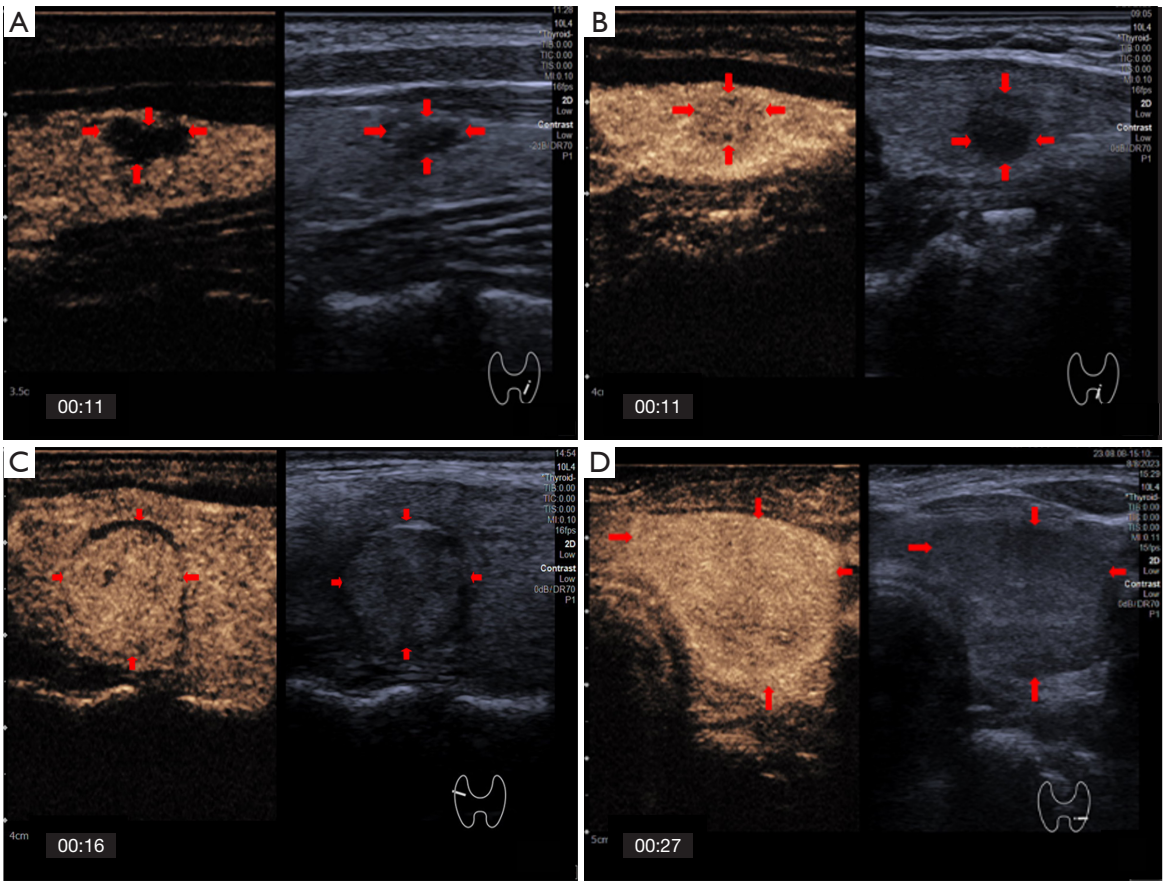

Figure 6 Images showing the feature of peak enhancement of thyroid nodules (red arrows). (A) Nonenhancement. (B) Hypoenhancement. (C) Isoenhancement. (D) Hyperenhancement. The minutes and seconds after the contrast media injection are indicated by the numbers in the bottom left corner of each panel.

they used the CEUS TI-RADS in the differential diagnosis of benign and malignant thyroid nodules, achieving good results in internal cross-validation and external validation; the ROCs were 0.93 (95% CI: 0.92–0.95) for internal validation, 0.89 (95% CI: 0.84–0.92) for the first external validation set, and 0.90 (95% CI: 0.85–0.94) for the second external validation set. However, none of these validation sets were investigated in groups based on nodule size. Our study categorized the nodules into groups based on size to further investigate the diagnostic efficacy of CEUS TI-RADS. The World Health Organization (WHO) defines papillary thyroid microcarcinoma (PTMC) as a PTC with a maximum diameter of 1 cm (22). Although several major guidelines, including the ACR, recommend surveillance of subcentimeter nodules, many patients with suspicious subcentimeter nodules are subjected to FNA in China due to patient anxiety, physician preference, family history, and other factors (23). When the maximum diameter of the nodule exceeds 4 cm, the risk of capsular and vascular invasion, which converts follicular adenoma into follicular carcinoma, increases, with the trachea being more likely to compress, causing aesthetic problems (1). Therefore, in our study, the nodules were classified based on their sizes (size ≤1 cm = group A, size >1 cm and ≤4 cm = group B, and size >4 cm = group C).

Our results revealed that the highest AUC of 0.949 (95% CI: 0.916–0.971, P<0.05) was obtained for nodules in group B, whereas the AUCs for nodules in groups A and group C were 0.795 (95% CI: 0.721–0.857, P<0.05) and 0.801 (95% CI: 0.644–0.910, P<0.05), respectively. This was consistent with the findings of Li *et al.* (24), who used CEUS to diagnose nodules smaller than 1 cm, reporting no significant benefit of CEUS in TMC diagnosis. The poor diagnostic efficacy of CEUS TI-RADS for subcentimeter nodules

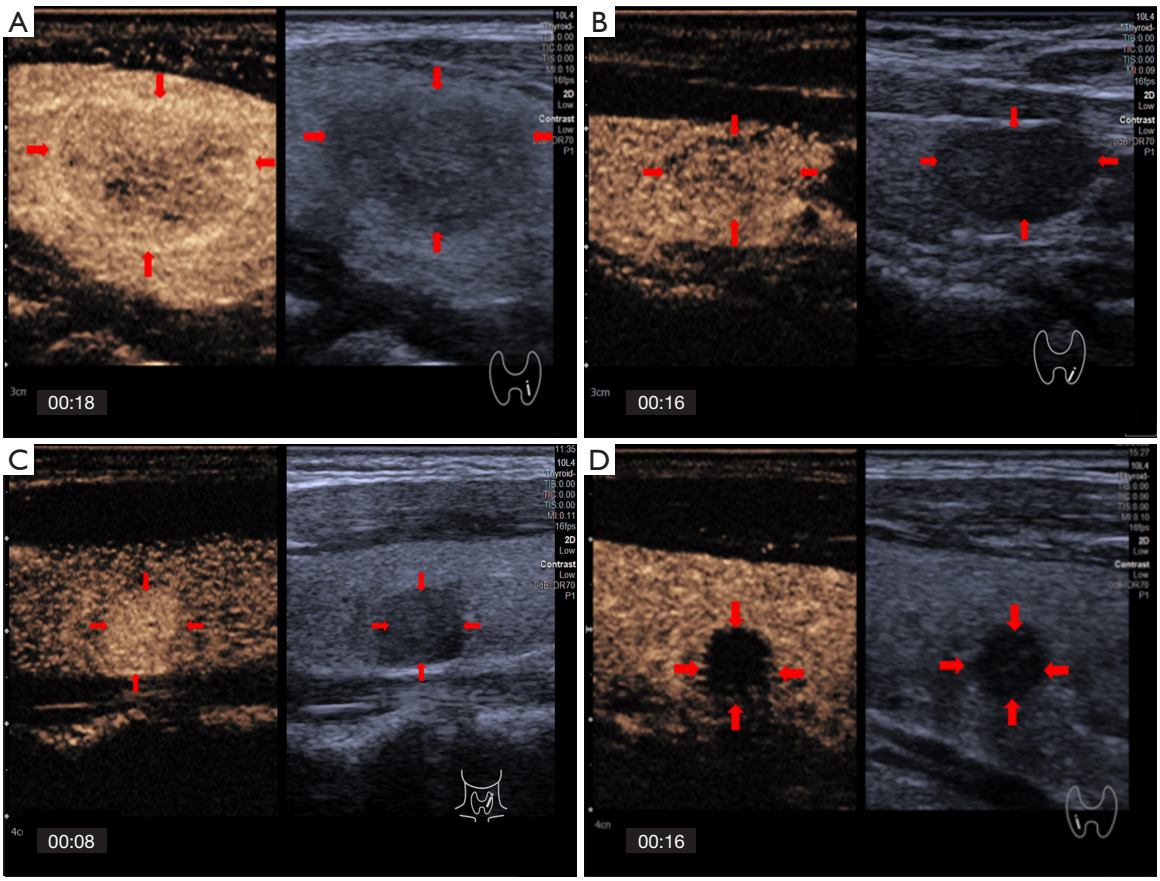

Figure 7 Images showing features of ring enhancement and composition of thyroid nodules (red arrows). (A) Ring enhancement. (B) Lack of ring enhancement. (C) Solid. (D) Nonsolid. The minutes and seconds since the contrast media injection are indicated by the numbers in the bottom left corner of each panel.

might be attributed to the following. First, suboptimal FNA due to issues of insufficient specimen size and false-negative results limit efficacy, with the bulk of related studies reporting false-negative rates of less than 5% and others reporting higher rates (ranging from 7.5% to 21%) (25). Second, a volume effect can arise in CEUS due to a small nodule size, which can lead to benign nodules, including mummified nodules, being easily misdiagnosed as malignant nodules. Therefore, we suggest that for subcentimeter nodules, the contrast agent dose could be appropriately reduced based on device conditions and the sonographer's experience to significantly minimize the volume effect. Nevertheless, when the nodule is too large for the limited probe exploration range, it is difficult to precisely diagnose the nodule, whereas CEUS could provide effective guidance for puncture to improve the positive puncture rate of nodules (26).

For the small-nodule (group A), the malignant nodules were mostly PTC, whereas the benign nodules were mainly nodular goiter. Both benign and malignant nodules were largely hypoechoic, with little evident extrathyroidal invasion, and most did not have ring enhancement features on CEUS. However, not all benign nodules in the large-nodule (group C) were predominantly iso/hypoechoic, and there were quite a few with hypoechoic features. Due to the large size, most of the nodules were wider than tall on conventional US, and nearly all appeared solid on CEUS. Due to the high number of vasculatures, branches, and arteriovenous fistulae inside the larger nodules, the inside of the nodule was simultaneously perfused with the blood-rich thyroid tissue, thus yielding unsatisfactory results in the differential diagnosis of benign and malignant large and small nodules via US and CEUS.

We found that CEUS TI-RADS had a significant benefit

Table 4 US and CEUS features of benign and malignant nodules of different sizes

US and CEUS features	Group A			Group B			Group C		
	Benign (n=69)	Malignant (n=79)	P	Benign (n=109)	Malignant (n=170)	P	Benign (n=27)	Malignant (n=13)	P
Echogenicity on US			0.009			<0.001			0.171
Hypoechoic	58 (84.1)	76 (96.2)		54 (49.5)	163 (95.9)		9 (33.3)	8 (61.5)	
Highly hypoechoic	2 (2.9)	2 (2.5)		1 (0.9)	1 (0.6)		0 (0.0)	0 (0.0)	
Hyper/isoechoic	9 (13.0)	1 (1.3)		54 (49.5)	6 (3.5)		18 (66.7)	5 (38.5)	
Shape on US			0.010			<0.001			>0.999
Wider than taller	40 (58.0)	29 (36.7)		101 (92.7)	87 (51.2)		25 (92.6)	12 (92.3)	
Taller than wide	29 (42.0)	50 (63.3)		8 (7.3)	83 (48.8)		2 (7.4)	1 (7.7)	
Echogenic foci on US			<0.001			<0.001			<0.001
No calcification	32 (46.5)	17 (21.5)		77 (70.6)	19 (11.2)		23 (85.2)	2 (15.4)	
Macrocalcification	13 (18.8)	6 (7.6)		21 (19.3)	17 (10.0)		4 (14.8)	3 (23.1)	
Rim calcification	3 (4.3)	1 (1.3)		0 (0.0)	1 (0.6)		0 (0.0)	1 (7.7)	
Punctate echogenic foci	21 (30.4)	55 (69.6)		11 (10.1)	133 (78.2)		0 (0.0)	7 (53.8)	
Margin on US			0.050			<0.001			0.048
Smooth or ill-defined	65 (94.2)	65 (82.3)		104 (95.4)	97 (57.1)		25 (92.6)	8 (61.5)	
Irregular or lobulated	4 (5.8)	14 (17.7)		5 (4.6)	73 (42.9)		2 (7.4)	5 (38.5)	
Extrathyroidal extension on US			0.306			<0.001			0.002
Present	3 (4.3)	8 (10.1)		0 (0.0)	51 (30.0)		0 (0.0)	5 (38.5)	
Absent	66 (95.7)	71 (89.9)		109 (100.0)	119 (70.0)		27 (100.0)	8 (61.5)	
Enhancement direction on CEUS			<0.001			<0.001			0.845
Scattered	16 (23.2)	0 (0.0)		22 (20.2)	10 (5.9)		6 (22.2)	4 (30.8)	
Centripetal/centrifugal	53 (76.8)	79 (100.0)		87 (79.8)	160 (94.1)		21 (77.8)	9 (69.2)	
Peak intensity on CEUS			<0.001			<0.001			0.002
None/isoenhancement	30 (43.5)	7 (8.9)		65 (59.6)	8 (4.7)		20 (74.1)	3 (23.0)	
Hypoenhancement	34 (49.3)	70 (88.6)		18 (16.5)	148 (87.1)		2 (7.4)	6 (46.2)	
Hyperenhancement	5 (7.2)	2 (2.5)		26 (23.9)	14 (8.2)		5 (18.5)	4 (30.8)	
Ring enhancement on CEUS			0.878			<0.001			0.023
Absent	66 (95.7)	77 (97.5)		45 (41.3)	160 (94.1)		7 (25.9)	9 (69.2)	
Present	3 (4.3)	2 (2.5)		64 (58.7)	10 (5.9)		20 (74.1)	4 (30.8)	
Composition on CEUS			<0.001			0.043			>0.999
Solid	58 (84.1)	79 (100.00)		101 (92.7)	167 (98.2)		26 (96.3)	13 (100.0)	
Nonsolid	11 (15.9)	0 (0.00)		8 (7.3)	3 (1.8)		1 (3.7)	0 (0.0)	

Data are presented as n (%). The nodules were grouped based on their size as follows: size ≤1 cm, group A; size >1 and ≤4 cm, group B; and size >4 cm, group C. US, ultrasound; CEUS, contrast-enhanced ultrasound.

in the differential diagnosis of thyroid mummification and PTC. Mummified thyroid nodules (MTNs) are cystic solid nodules that change after treatment via processes such as resorption or nodal ablation. These nodules show signs of malignancy on US, including hypoechoicity or high hypoechoicity and taller-than-wide shape in atrophic collapse, which may indicate TI-RADS 5 in the ACR TI-RADS classification (27). Furthermore, we discovered that CEUS could improve the classification between PTC and MTNs, as 85.5% (224/262) of PTCs exhibited centripetal or centrifugal hypoenhancement due to relatively poor vascularization (*Figures 4*,*5A-5C*). On the other hand, the majority of MTNs did not show enhancement on CEUS (*Figures 6A*,*7D*), and this observation might help improve the diagnostic efficacy of ACR TI-RADS and reduce the unnecessary FNA or surgical resections of MTNs. This result is consistent with the findings of Chen *et al.* (28).

Although CEUS may play a crucial role in differentiating MTNs from PTCs, this scoring system failed to categorize FTC and inflammatory nodules. In our study, there were 6 cases of FTC, among which only 2 cases were classified as category 5 and 4 as categories 3–4A; circumferential hyperenhancement was observed in the 6 cases of FTC. Therefore, distinguishing FTC from adenoma or nodular goiter with adenomatous hyperplasia was difficult because the US manifestations of FTC did not show apparent malignant signs, including extrathyroidal invasion or microcalcifications. Since tumor invasion of the margin or blood vessels is the only pathological diagnostic criterion for FTC (29), CEUS TI-RADS could not differentiate between FTC and FTA with any degree of precision. Therefore, there is a need for additional studies on CEUS SEN and SPE for FTC diagnosis.

Meanwhile, 5 nodules with Hashimoto's thyroiditis pathology and 2 nodules with granulomatous thyroiditis pathology were misdiagnosed as malignant. The misdiagnoses were attributed to the concomitant microcalcification of the nodules, an aspect ratio >1, and low enhancement of the malignant signs. Hashimoto's thyroiditis with fibrosclerotic nodules and granulomatous thyroiditis is characterized by a primary pathological change of fibrosis and poor blood supply. These features tend to overlap on US and CEUS, hence complicating these conditions' differentiation from malignant nodules (30). Zhang *et al.* (30) demonstrated that CEUS combined with time-intensity curve (TIC) parameters could provide effective quantitative information on microvascular perfusion for the differential diagnosis of inflammatory thyroid nodules and PTC, which warrants further validation.

Unlike the results of Ruan *et al.* (15), our study performed logistic regression analysis of the US and CEUS characteristics of 467 nodules, in which only 1 independent risk factor was correlated with CEUS, while the rest were correlated with US. This might be explained by the fact that hypoenhancement in CEUS is obvious in most nodules, while the US characteristics are needed to differentiate small-sized malignant nodules. Moreover, we found that hyperenhancement and the presence or absence of circumferential enhancement were not statistically significant in differentiating between benign and malignant nodules, which is consistent with the findings of many previous studies (9,24,31). We believe that the inconsistent conclusions might still be attributed to the tumor size and growth stage. Tumor growth is categorized into two stages: from the slow growth stage without blood vessels (prevascular stage) to the rapid growth stage with blood vessels (vascular stage). In our study, for relatively small tumors with no or few blood vessels, the enhancement observed by CEUS was primarily hypoenhancement. Upon rapid tumor growth, a diversity of neovascularization forms due to various angiogenic factors, causing the nodule hyperenhancement that is apparent on CEUS (32). Notably, the presence of a halo is often considered a benign feature (33). However, some thin halos appearing on conventional US might be unclear and difficult to detect, whereas the surrounding rings could be observed on CEUS. A greater number of peripheral halo rings can be observed on CEUS than on conventional US. Due the factors leading to formation of ring enhancement in nodules being unclear, some researchers (34,35) analyzed this feature and have proposed that irregular ring hyperenhancement is a sign of malignancy; meanwhile, a enhanced ring with regularity or irregularity should be combined with the enhancement features inside the nodules. Therefore, we speculated that categorizing ring enhancement before allocating points could be more rigorous.

In our study, a senior and a junior medical practitioner independently assessed 150 thyroid nodules, using the CEUS TI-RADS classification system for scoring purposes. The ICC was 0.86, indicating a high degree of consistency in their assessments. This outcome confirmed the use of this approach as a valuable diagnostic tool for junior medical practitioners.

This work has several noteworthy limitations. First, we employed a single-center, retrospective design, and the reading scores of the physicians were based on static charts, which did not mimic real clinical practice; thus, the findings

might not be generalizable to other institutions. Second, some of our pathology outcomes were based on FNA, which could have potentially involved false positives and false negatives. Third, most of the malignant nodules were PTCs; therefore, the diagnostic value of this scoring system needs to be assessed for other malignant pathologic types.

Conclusions

The novel CEUS TI-RADS scoring system has high efficacy in the differential diagnosis of benign and malignant thyroid nodules and may potentially help reduce the number of FNA procedures or unnecessary surgical interventions for benign nodules, particularly MTNs. Moreover, its diagnostic efficacy was influenced by the nodule size, and the optimal performance was in nodules with sizes between 1 to 4 cm. These observations may provide valuable information for clinical diagnosis and treatment.

Acknowledgments

The authors would like to thank the Clinical Trials Service Center of the Affiliated Hospital of Guangdong Medical University for assistance with the statistical analyses.
Funding: This work was supported by the Innovation and Practice Training Model for Professional Degree Postgraduates and the Graduate Teaching Reform Research Project of the Affiliated Hospital of Guangdong Medical University.

Footnote

Reporting Checklist: The authors have completed the STARD reporting checklist. Available at https://qims.amegroups.com/article/view/10.21037/qims-24-457/rc

Conflicts of Interest: All authors have completed the ICMJE uniform disclosure form (available at https://qims.amegroups.com/article/view/10.21037/qims-24-457/coif). The authors have no conflicts of interest to declare.

Ethical Statement: The authors are accountable for all aspects of the work in ensuring that questions related to the accuracy or integrity of any part of the work are appropriately investigated and resolved. This study was conducted in accordance with the Declaration of Helsinki (as revised in 2013) and was approved by the ethics review board of Affiliated Hospital of Guangdong Medical University (No. PJKT2024-028). Informed consent was provided by all participants.

References

1. Alexander EK, Doherty GM, Barletta JA. Management of thyroid nodules. Lancet Diabetes Endocrinol 2022;10:540-8.
2. Durante C, Grani G, Lamartina L, Filetti S, Mandel SJ, Cooper DS. The Diagnosis and Management of Thyroid Nodules: A Review. JAMA 2018;319:914-24.
3. Horvath E, Majlis S, Rossi R, Franco C, Niedmann JP, Castro A, Dominguez M. An ultrasonogram reporting system for thyroid nodules stratifying cancer risk for clinical management. J Clin Endocrinol Metab 2009;94:1748-51.
4. Kwak JY, Han KH, Yoon JH, Moon HJ, Son EJ, Park SH, Jung HK, Choi JS, Kim BM, Kim EK. Thyroid imaging reporting and data system for US features of nodules: a step in establishing better stratification of cancer risk. Radiology 2011;260:892-9.
5. Russ G, Bonnema SJ, Erdogan MF, Durante C, Ngu R, Leenhardt L. European Thyroid Association Guidelines for Ultrasound Malignancy Risk Stratification of Thyroid Nodules in Adults: The EU-TIRADS. Eur Thyroid J 2017;6:225-37.
6. Tessler FN, Middleton WD, Grant EG, Hoang JK. Re: ACR Thyroid Imaging, Reporting and Data System (TI-RADS): White Paper of the ACR TI-RADS Committee. J Am Coll Radiol 2018;15:381-2.
7. Zhou J, Yin L, Wei X, Zhang S, Song Y, Luo B, et al. 2020 Chinese guidelines for ultrasound malignancy risk stratification of thyroid nodules: the C-TIRADS. Endocrine 2020;70:256-79.
8. Radzina M, Ratniece M, Putrins DS, Saule L, Cantisani V. Performance of Contrast-Enhanced Ultrasound in Thyroid Nodules: Review of Current State and Future

Perspectives. Cancers (Basel) 2021;13:5469.
9. Huang K, Bai Z, Bian D, Yang P, Li X, Liu Y. Diagnostic Accuracy of Contrast-Enhanced Ultrasonography in Papillary Thyroid Microcarcinoma Stratified by Size. Ultrasound Med Biol 2020;46:269-74.
10. Zhou P, Chen F, Zhou P, Xu L, Wang L, Wang Z, Yu Y, Liu X, Wang B, Yan W, Zhou H, Tao Y, Liu W. The use of modified TI-RADS using contrast-enhanced ultrasound features for classification purposes in the differential diagnosis of benign and malignant thyroid nodules: A prospective and multi-center study. Front Endocrinol (Lausanne) 2023;14:1080908.
11. Zhang J, Zhang X, Meng Y, Chen Y. Contrast-enhanced ultrasound for the differential diagnosis of thyroid nodules: An updated meta-analysis with comprehensive heterogeneity analysis. PLoS One 2020;15:e0231775.
12. Zhan J, Ding H. Application of contrast-enhanced ultrasound for evaluation of thyroid nodules. Ultrasonography 2018;37:288-97.
13. Liu Z, Li C. Correlation of lymph node metastasis with contrast-enhanced ultrasound features, microvessel density and microvessel area in patients with papillary thyroid carcinoma. Clin Hemorheol Microcirc 2022;82:361-70.
14. Xiao L, Zhou J, Tan W, Liu Y, Zheng H, Wang G, Zheng W, Pei X, Yang A, Liu L. Contrast-enhanced US with Perfluorobutane to Diagnose Small Lateral Cervical Lymph Node Metastases of Papillary Thyroid Carcinoma. Radiology 2023;307:e221465.
15. Ruan J, Xu X, Cai Y, Zeng H, Luo M, Zhang W, Liu R, Lin P, Xu Y, Ye Q, Ou B, Luo B. A Practical CEUS Thyroid Reporting System for Thyroid Nodules. Radiology 2022;305:149-59.
16. Cavallo A, Johnson DN, White MG, Siddiqui S, Antic T, Mathew M, Grogan RH, Angelos P, Kaplan EL, Cipriani NA. Thyroid Nodule Size at Ultrasound as a Predictor of Malignancy and Final Pathologic Size. Thyroid 2017;27:641-50.
17. Zhao L, Yan H, Pang P, Fan X, Jia X, Zang L, Luo Y, Wang F, Yang G, Gu W, Du J, Wang X, Lyu Z, Dou J, Mu Y. Thyroid nodule size calculated using ultrasound and gross pathology as predictors of cancer: A 23-year retrospective study. Diagn Cytopathol 2019;47:187-93.
18. Sugitani I, Ito Y, Takeuchi D, Nakayama H, Masaki C, Shindo H, Teshima M, Horiguchi K, Yoshida Y, Kanai T, Hirokawa M, Hames KY, Tabei I, Miyauchi A. Indications and Strategy for Active Surveillance of Adult Low-Risk Papillary Thyroid Microcarcinoma: Consensus Statements from the Japan Association of Endocrine Surgery Task Force on Management for Papillary Thyroid Microcarcinoma. Thyroid 2021;31:183-92.
19. Frasca F, Piticchio T, Le Moli R, Tumino D, Cannavò S, Ruggeri RM, Campennì A, Giovanella L. Early detection of suspicious lymph nodes in differentiated thyroid cancer. Expert Rev Endocrinol Metab 2022;17:447-54.
20. Cibas ES, Ali SZ. The 2017 Bethesda System for Reporting Thyroid Cytopathology. Thyroid 2017;27:1341-6.
21. Zhang Y, Lu F, Shi H, Guo LH, Wei Q, Xu HX, Zhang YF. Predicting malignancy in thyroid nodules with benign cytology results: The role of Conventional Ultrasound, Shear Wave Elastography and BRAF V600E. Clin Hemorheol Microcirc 2022;81:33-45.
22. Lloyd RV, Osamura RY, Klöppel G, Rosai J. WHO classification of tumours of endocrine organs. WHO Classification of Tumours, 4th Edition, 2017.
23. Hussain N, Goldstein MB, Zakher M, Katz DS, Brandler TC, Islam S, Rothberger GD. Proportion of Malignancy and Evaluation of Sonographic Features of Thyroid Nodules Classified as Highly Suspicious Using ACR TI-RADS Criteria. J Ultrasound Med 2023;42:443-51.
24. Li F, Zhang J, Wang Y, Liu L. Clinical value of elasticity imaging and contrast-enhanced ultrasound in the diagnosis of papillary thyroid microcarcinoma. Oncol Lett 2015;10:1371-7.
25. Zhu Y, Song Y, Xu G, Fan Z, Ren W. Causes of misdiagnoses by thyroid fine-needle aspiration cytology (FNAC): our experience and a systematic review. Diagn Pathol 2020;15:1.
26. Todsen T, Bennedbaek FN, Kiss K, Hegedüs L. Ultrasound-guided fine-needle aspiration biopsy of thyroid nodules. Head Neck 2021;43:1009-13.
27. Lacout A, Chevenet C, Marcy PY. Mummified Thyroid Syndrome. AJR Am J Roentgenol 2016;206:837-45.
28. Chen S, Tang K, Gong Y, Ye F, Liao L, Li X, Zhang Q, Xu Y, Zhang R, Niu C. Value of Contrast-Enhanced Ultrasound in Mummified Thyroid Nodules. Front Endocrinol (Lausanne) 2022;13:850698.
29. He Y, Wang XY, Hu Q, Chen XX, Ling B, Wei HM. Value of Contrast-Enhanced Ultrasound and Acoustic Radiation Force Impulse Imaging for the Differential Diagnosis of Benign and Malignant Thyroid Nodules. Front Pharmacol 2018;9:1363.
30. Zhang P, Liu H, Yang X, Pang L, Gu F, Yuan J, Ding L, Zhang J, Luo W. Comparison of contrast-enhanced ultrasound characteristics of inflammatory thyroid nodules and papillary thyroid carcinomas using a quantitative time-intensity curve: a propensity score matching analysis.

Quant Imaging Med Surg 2022;12:5209-21.
31. Huang Y, Hong Y, Xu W, Song K, Huang P. Contrast-Enhanced Ultrasound Improves the Accuracy of the ACR TI-RADS in the Diagnosis of Thyroid Nodules Located in the Isthmus. Ultraschall Med 2022;43:599-607.
32. Yuan Z, Quan J, Yunxiao Z, Jian C, Zhu HE. Association between real-time contrast-enhanced ultrasound characteristics and thyroid carcinoma size. Mol Clin Oncol 2015;3:743-6.
33. Propper RA, Skolnick ML, Weinstein BJ, Dekker A. The nonspecificity of the thyroid halo sign. J Clin Ultrasound 1980;8:129-32.
34. Zhang Y, Zhang MB, Luo YK, Li J, Wang ZL, Tang J. The Value of Peripheral Enhancement Pattern for Diagnosing Thyroid Cancer Using Contrast-Enhanced Ultrasound. Int J Endocrinol 2018;2018:1625958.
35. Zhang Y, Luo YK, Zhang MB, Li J, Li J, Tang J. Diagnostic Accuracy of Contrast-Enhanced Ultrasound Enhancement Patterns for Thyroid Nodules. Med Sci Monit 2016;22:4755-64.

Cite this article as: Yang YP, Zhang GL, Zhou HL, Dai HX, Huang X, Liu LJ, Xie J, Wang JX, Li HJ, Liang X, Yuan Q, Zeng YH, Xu XH. Diagnostic efficacy of the contrast-enhanced ultrasound thyroid imaging reporting and data system classification for benign and malignant thyroid nodules. Quant Imaging Med Surg 2024;14(8):5721-5736. doi: 10.21037/qims-24-457

